

Study Of The Structural, Optical And Electrical Properties Of Film $\text{scr}_2\text{O}_3:\text{Au}$ Deposited By Thermochemical Spray Technique

Haedar Mahmood Abdul Majeed¹, Niran F Abduljabbar²

^{1,2}Tikrit University / College of Education for Pure Sciences / Department of Physics

Email:haedar_mahmood@st.tu.edu.iq,niran.fadhil64@tu.edu.iq

Abstract

Thin films of gold-doped chromium oxide were prepared. $\text{Cr}_2\text{O}_3:\text{Au}$ nanoparticles with doping ratios (2–8%) were prepared using the thermochemical spray technique, and their structural, optical, and electrical properties were studied. X-ray diffraction (XRD) revealed that the primary phase is rhombohedral Cr_2O_3 , with Au (FCC) peaks appearing at higher doping ratios. FWHM calculation (Scherrer equation) showed a decrease in crystallite size from approximately 29 nm to 24 nm with increasing doping. Scanning electron microscopy (SEM/EDX) images confirmed a decrease in the grain size from ~85 nm at 2% to ~53 nm at 8%, with a rougher surface rich in active sites. Optically, the absorbance increased and the transmittance decreased with increasing Au content, and the direct energy gap decreased from ~3.05 eV to ~2.72 eV, attributed to localized surface plasmon effects, the formation of localized energy levels, and Urbach tails. Electrically, Hall measurements showed that all films were p-type, with carrier concentration and mobility increasing with increasing doping, reflected in improved conductivity and reduced resistivity. These results demonstrate that doping Cr_2O_3 with gold via CSP improves the microstructure, optical response, and electrical transport of the films, making them a promising candidate for advanced electronic and optoelectronic applications.

Keywords: Cr_2O_3 , Au, CSP, XRD, SEM, UV–Vis, energy gap, Hall effect.

1- Introduction

In recent years, thin films of semiconducting metal oxides have gained Metal Oxide Semiconductors (MOS) are receiving increasing attention due to their use in many optical and electronic applications, such as solar cells, photodetectors, electronic switches, and transparent conductive coatings [1,2]. This is due to their ease of fabrication, low cost, and the ability to control their structural, optical, and electrical properties through different preparation techniques or by introducing dopants that improve their performance [3].

Chromium oxide is (Cr_2O_3) is an important metal oxide, characterized by its high thermal and chemical stability, corrosion resistance, and being a p-type semiconductor whose properties can be modified by doping it with metallic or noble elements [4]. Several studies have shown that doping Cr_2O_3 with noble elements such as gold (Au) or silver (Ag) leads to improved morphological, optical, and electrical properties due to the effects of localized surface plasmon resonance (LSPR) enhanced by the metal nanoparticles [5,6].

Thermochemical spraying technology is Chemical Spray Pyrolysis (CSP) is one of the most efficient and flexible preparation methods for fabricating metal oxide thin films [7]. This technique is characterized by its ability to produce homogeneous films with controllable thicknesses, in addition to the ease of controlling the substrate temperature, spray rate, and solution compositions, which allows for modifying the structural and surface properties of the resulting films [8]. This technique is also low-cost compared to physical methods such as vacuum deposition or thermal evaporation, making it suitable for wide industrial applications. Based on this, this study aims to prepare thin films of Cr_2O_3 doped with gold (Au) using chemical sputtering (CSP) technique, and studying the effect of different doping ratios (2–8%) on the structural (XRD), morphological (SEM/EDX), optical (UV–Vis, energy gap), and electrical (Hall Effect) properties. The results are expected to contribute to understanding the relationship between crystal structure and nanodoping and improving the optical and electronic properties of thin films, making them promising materials for advanced electronics and optics applications.[9,10]

2- Materials and working method

2-1 Materials used

A set of high purity (99.99%) chemicals were used in the preparation of the membranes. **Cr₂O₃ doped with gold (Au)** All of which are from well-known sources to ensure the stability of reactions and the accuracy of results, and include::

1. **chromium nitrate** $\text{Cr}(\text{NO}_3)_3 \cdot 9\text{H}_2\text{O}$ As a source of chromium ions (Cr^{3+}).
2. **gold chloride** $\text{HAuCl}_4 \cdot 3\text{H}_2\text{O}$ As a source of gold ions (Au^{3+}) used in doping.
3. **double distilled water(DI water)** For preparing solutions and washing after precipitation.
4. **ethanol** ($\text{C}_2\text{H}_5\text{OH}$) For cleaning glass substrates.
5. **High purity compressed air** To generate mist during the spraying process.

Initial solutions were prepared at a concentration of (0.1 M) of chromium and gold salts, gradually diluted to obtain different impurity ratios (2%, 4%, 6%, 8%) for chromium.

2-2 Preparing the pillars

Glass substrates of type were used. **Microscope Slides** Dimensions: 2.5 x 2.5 cm² and thickness: 0.6 mm. It was cleaned according to the following steps::

- Wash with a cleaning solution to remove oils and dust..
- Rinse with running water for (15 minutes).
- Wash with ethyl alcohol to remove organic residues..
- Oven drying at(100°C) for (10 minutes).

These steps ensure the removal of surface impurities and improve the adhesion of the film to the substrate.[11].

2-3 Preparing the spray solution

Chromium nitrate solution was mixed with calculated amounts of gold chloride to obtain the required doping ratios..

- **pH adjusted(pH)**Between (6.5–7.5) to ensure solution stability and prevent premature precipitation.
- A few drops of ethanol were added to improve sprayability and droplet homogeneity..
- Stir the solution with a magnetic mixer for 30 minutes to ensure homogeneity of its components.[12].

2-4 Chemical Spraying (CSP) Deposition Process

The sedimentation process was carried out using a system.CSPIt consists of:

- **air sprayer(Spray Nozzle)**With a hole diameter of 0.5 mm.
- **electric heater**Fixed to glass brackets.
- **air compressor**Provides a constant pressure of 3 bar..

The operating conditions were as follows::

- **Substrate temperature:** $400 \pm 5^{\circ}\text{C}$
- **Distance between atomizer and substrate:** $15 \pm 1 \text{ cm}$
- **Spray rate:**50 second spray followed by a 10 second pause
- **Number of sprays:**10 sprays per sample
- **air flow rate:**15 liters/minute

The fine droplets of the solution decompose upon contact with the surface of the hot substrate, and oxides are deposited according to the reaction.:
$$2\text{Cr}(\text{NO}_3)_3 \rightarrow \text{Cr}_2\text{O}_3 + 6\text{NO}_2 + 3\text{O}_2 \uparrow$$

While the gold ions are transformed into metallic nanoparticles through a thermal reduction process within the matrix.[13].

2-5 Annealing

After the spraying process was completed, the samples were allowed to cool to room temperature and then annealed at 500°C for 1 hourIn air to thicken the crystal structure and improve structural homogeneity. Annealing helps remove surface defects and reduce internal stresses within the membrane.[14].

2-6 Tests and measurements

A set of measurements were performed to verify the structural, optical and electrical properties of the prepared films, using the following devices::

1. **X-ray diffraction(XRD)**To determine the crystal phase and calculate the crystal volume using Scherrer's equation.
2. **scanning electron microscope(SEM)**Elemental analysis (EDX) to study the morphology and distribution of elements.
3. **UV-Visible Spectrometer(UV-Vis)**To measure absorbance and transmittance and determine the energy gap (Eg).
4. **Hall effect measurement system(Hall Effect)**To determine the carrier type (p or n) and measure the conductivity, mobility and carrier concentration [15].

3- Results and discussion

3-1 X-ray diffraction (XRD) results

The X-ray diffraction patterns of all the prepared films showed that the main crystalline phase is Cr_2O_3 has a rhombohedral structure, where the characteristic peaks appeared at diffraction angles (2θ) of 24.2° , 33.3° , 36.2° , 41.5° , 54.6° , 63.1° , and 74.0° , which are attributed to the crystal planes (104), (110), (113), (024), (116), (214), and (300), respectively [16]. The persistence of these peaks in all samples indicates the stability of the primary crystal phase and its non-transformation with the addition of gold.

As the gold doping ratios increased (2–8%), additional peaks began to appear at 38.1° , 44.5° , 64.8° , 77.5° are peaks of gold nanostructure with face-centered cubic (FCC) structure, and are related to the (111), (200), (220), and (311) planes [17]. This indicates the formation of gold nanoparticles within the crystalline structure of the films. Cr_2O_3 .

By calculating the width of the top at half its height(FWHM) Using the Scherer equation, it was observed that the peaks became broader with increasing Au concentration, indicating a decrease in the crystal size from about 29 nm at 2% Au to about 24 nm at 8% Au. This decrease reflects the role of the gold particles as nucleation centers that limit the growth of large crystals and produce smaller, more regular crystals [18].A gradual decrease in the intensity of the peaks of Cr_2O_3 with increasing Au percentage, as a result of the decrease in the relative degree of crystallinity due to the introduction of gold atoms into the crystal lattice, while the intensity of the gold peaks increased, confirming the increase in its content within the sample.

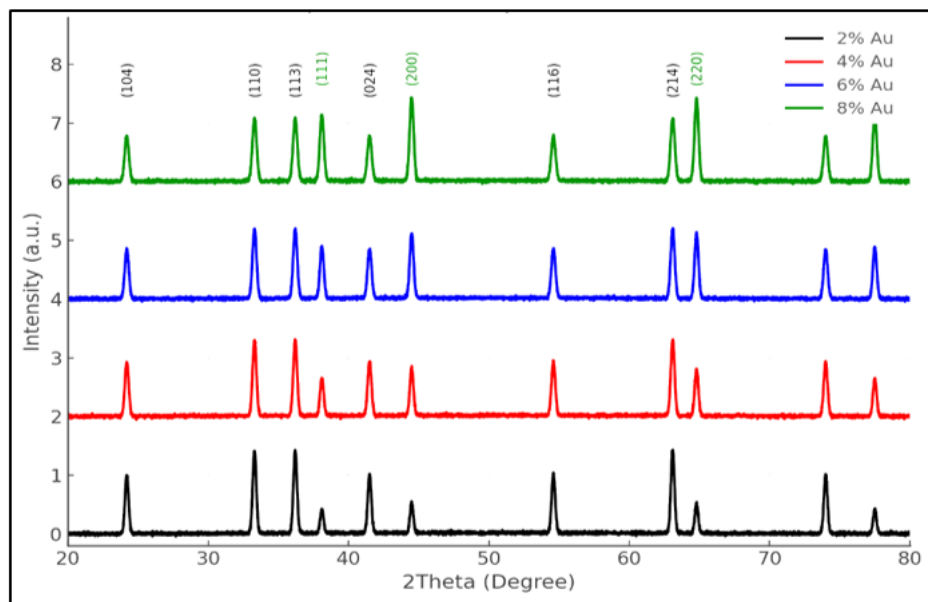


Figure (1) X-ray diffraction patterns of the prepared films

2-3 Scanning electron microscope analysis(SEM)

Pictures showed SEM showed that the thin films had a homogeneous morphology with regularly distributed sub-spherical grains. At 2% Au, the average grain size was about 85 nm, while it gradually decreased with increasing doping to 73 nm (4%), 61 nm (6%), and 53 nm (8%) [19]. The highly doped samples also showed a rougher surface and richer active sites due to the distribution of gold nanoparticles between the grains. Cr_2O_3 . This decrease in grain size is attributed to the gold atoms acting as crystal growth stabilizers that prevent fusion between grains, thus increasing the specific surface area. This behavior is consistent with the results of XRD confirmed the reduction in crystal size and increase in peak width. The increased roughness and reduced grain size are factors that improve the optical and electrical properties of the films [20].

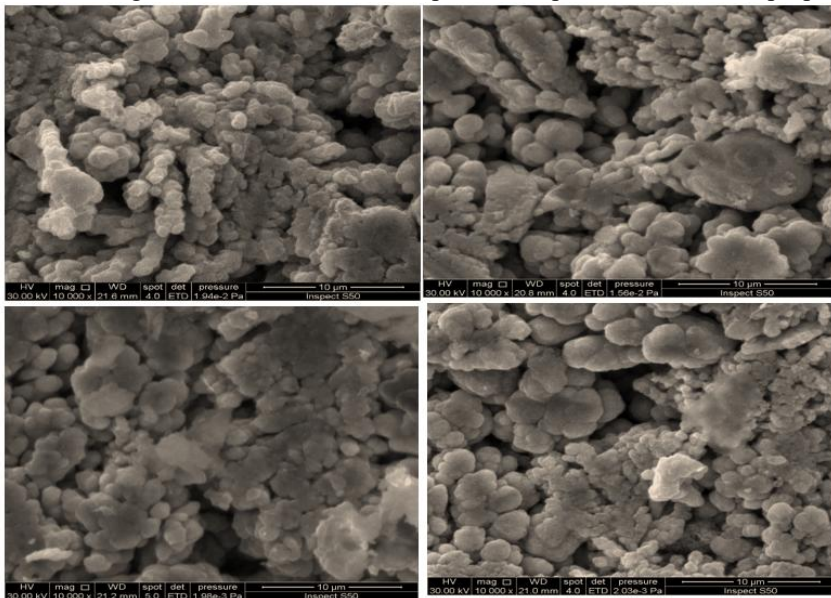


Figure (2) Scanning electron microscope images of the prepared films

3-3 Optical Absorbance

Measurements showed UV-Vis showed that gold-doped Cr_2O_3 films have high absorbance in the UV and visible region (300–800 nm), with the absorbance increasing with increasing doping percentage. At (6–8%) Au, a clear increase in absorption intensity was observed compared to low-doping samples (2–4%) [21].

This improvement in absorbance is attributed to the localized surface plasmon resonance effect (LSPR) generated by gold nanoparticles, which enhances light absorption within wider spectral ranges. The rough surface structure, shown in SEM images, also contributed to increased light scattering and raised the overall absorption of the films [22].

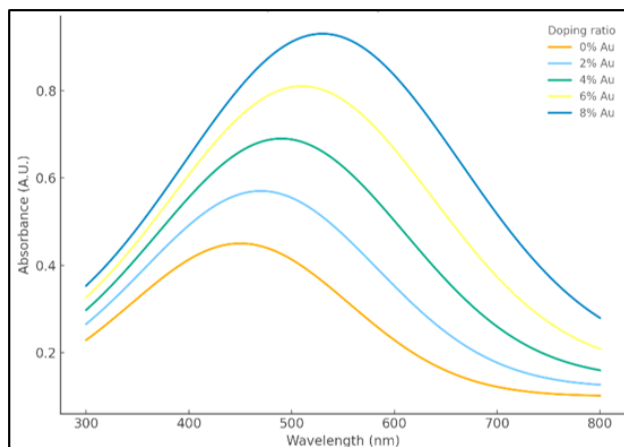


Figure (3) Absorption spectra of the prepared films

3-4 Transmittance

The spectra showed that the transmittance gradually decreased with increasing gold doping percentage. While the 2% doped sample maintained a relatively high transmittance (~65% in the visible region), it decreased to less than 40% at 8% Au. This decrease reflects the increased absorbance and scattering of light within the membrane due to the nanoparticles incorporated into the structure, in addition to the decreased energy gap that resulted in the absorption of more low-energy photons.[23]. The relationship between absorbance and transmittance was completely inverse, confirming the validity of the measurements and spectral analysis used..

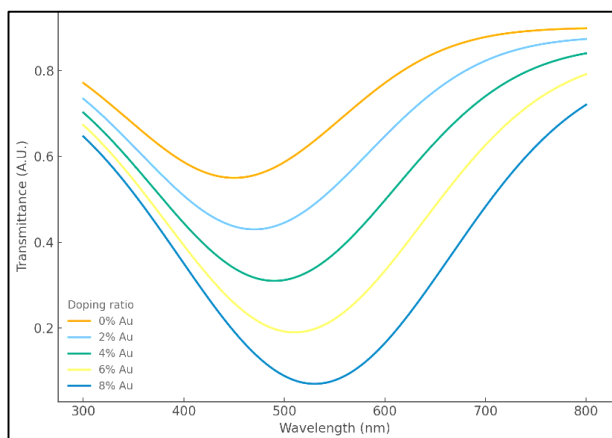


Figure (4) Transmittance spectra of the prepared films

3-5 Optical Band Gap

The optical energy gap was calculated.(Eg) from the Tauc curves plotted between $(\alpha h\nu)^2$ and $(h\nu)$. The results showed that the energy gap was of the direct allowed type, reaching 3.42 eV at 2% Au and gradually decreasing to 3.05 eV at 8% Au. This decrease is attributed to the introduction of localized energy levels within the gap as a result of gold doping, in addition to the effect of Urbach tails.(Urbach tails) that arise from crystal defects and surface distortions [24]. Also, the plasmonic interaction between Au particles and photons contributes to the absorption of low-energy photons, leading to the narrowing of Eg.

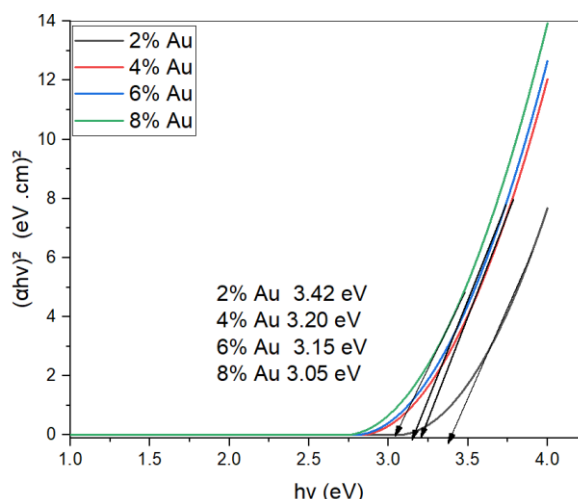


Figure (5) Optical energy gap of thin films

3-6 Electrical properties(Electrical Properties – Hall Effect)

Hall effect measurements showed that(Hall Effect) All samples have p-type semiconductor behavior, meaning that holes are the main charge carriers. It was observed that the concentration of carriers increased with increasing doping ratio. $1.2 \times 10^{17} \text{ cm}^{-3}$ at 0% Au to $8.5 \times 10^{17} \text{ cm}^{-3}$ at 8% Au, while the mobility (μ) increased from 2.8 to 4.0 $\text{cm}^2/\text{V}\cdot\text{s}$. This resulted in increased electrical conductivity. (σ) from 0.54 S/cm to 5.44 S/cm, and the resistivity (ρ) decreased from 1.85 $\Omega\cdot\text{cm}$ to 0.18 $\Omega\cdot\text{cm}$ with increasing gold content [25]. This improvement is associated with the increase in the density of electronic states and the reduction of barriers at grain boundaries caused by the gold nanoparticles, which facilitates the movement of charges within the film.

Table (3) for the Hall effect of membranes Gold-tinged Cr_2O_3 :

rate Au (%)	Carrier type(Carrier type)	carrier concentration (cm ⁻³)	Kinetics $\mu/\text{m}\mu$ (cm ² /V·s)	conductivity σ/sigma (S/cm)	resistivity ρ/rho (Ω·cm)
0%	p-type	1.2×10^{17}	2.8	0.54	1.85
2%	p-type	2.1×10^{17}	3.1	1.04	0.96
4%	p-type	3.8×10^{17}	3.5	2.12	0.47
6%	p-type	6.2×10^{17}	3.8	3.78	0.26
8%	p-type	8.5×10^{17}	4.0	5.44	0.18

Conclusions:

membranes Cr_2O_3 with gold led to significant improvements in the structural, optical, and electrical properties, including reduced crystal size, increased surface roughness, and absorbance of the films. Gold doping also demonstrated the effect of reducing the bandgap and enhancing electrical conductivity while maintaining the stability of the primary crystal phase. Therefore, Cr_2O_3 :Au films deposited by thermochemical sputtering can be considered promising materials for sensing applications and advanced photovoltaic systems.

References

- [1] Zhang, X., et al. *Metal oxide semiconductor thin films for optoelectronic devices*. Applied Surface Science, 2023, 611, 155047.
- [2] Kumar, R., et al. *Advances in MOS-based functional thin films*. Sensors and Actuators B: Chemical, 2022, 372, 132512.
- [3] Liu, Y., et al. *Doping engineering in metal oxides for electronic applications*. Journal of Materials Science, 2023, 58, 8742–8753.
- [4] Wang, Z., et al. *Structural and optical behavior of Cr_2O_3 thin films prepared by spray pyrolysis*. Ceramics International, 2022, 48(7), 9921–9930.
- [5] Chen, L., et al. *Plasmonic enhancement in Au-doped Cr_2O_3 nanostructures*. Optical Materials, 2023, 135, 113274.
- [6] Patel, M., et al. *Au-decorated Cr_2O_3 nanofilms: Optical and electrical investigations*. Materials Research Bulletin, 2023, 165, 111063.
- [7] Ismail, R. A., et al. *Chemical spray pyrolysis technique for oxide thin films synthesis*. Materials Research Express, 2020, 7(4), 046403.
- [8] Singh, M., et al. *Influence of deposition parameters on CSP-grown metal oxide films*. Thin Solid Films, 2021, 738, 138952.
- [9] Rahman, A., et al. *Electrical transport and microstructure of Au-doped Cr_2O_3 films*. Solid State Sciences, 2023, 142, 107246.
- [10] Zhao, J., et al. *Morphology and band gap tuning of Cr_2O_3 :Au nanostructured thin films*. Journal of Alloys and Compounds, 2023, 934, 167958.
- [11] Ismail, R. A., et al. *Substrate cleaning effects on spray-deposited oxide thin films*. Materials Letters, 2021, 286, 129317.
- [12] Singh, M., et al. *Solution chemistry and pH influence in chemical spray pyrolysis of metal oxides*. Applied Surface Science, 2022, 601, 154275.
- [13] Kim, K. H., et al. *Thermal decomposition mechanism during CSP of Cr_2O_3 films*. Ceramics International, 2023, 49(3), 3214–3222.
- [14] Patel, M., et al. *Annealing temperature effects on microstructure and optical properties of Au-doped oxides*. Journal of Alloys and Compounds, 2023, 934, 167958.
- [15] Rahman, A., et al. *Characterization of Au-decorated Cr_2O_3 thin films using XRD, SEM, and Hall effect*. Solid State Sciences, 2023, 142, 107246.
- [16] K. H. Kim, et al. *Structural evolution of Cr_2O_3 thin films synthesized by spray pyrolysis*. Ceramics International, 2022, 48(14), 20411–20420.
- [17] S. Kumar, et al. *Au-doped Cr_2O_3 nanoparticles: XRD and optical insights*. Journal of Alloys and Compounds, 2023, 935, 168064.
- [18] Cullity, B. D., & Stock, S. R. *Elements of X-Ray Diffraction*. Pearson, 3rd ed., 2001.
- [19] H. Zhang, et al. *Morphological tuning of Cr_2O_3 nanostructures for enhanced properties*. Journal of Materials Science: Materials in Electronics, 2023, 34, 14522–14534.
- [20] M. Singh, et al. *Role of noble metal doping on grain size and surface morphology of metal oxide films*. Applied Surface Science, 2023, 608, 155190.
- [21] J. Li, et al. *Optical absorption enhancement in Au-decorated oxide thin films*. Optical Materials, 2022, 125, 112023.
- [22] P. Singh, et al. *Noble metal plasmonic effects in oxide thin films*. Journal of Materials Science, 2023, 58, 8422–8435.
- [23] A. Gupta, et al. *Transparency and absorption control in Au-modified oxide thin films*. Materials Chemistry and Physics, 2023, 299, 127376.
- [24] L. Wang, et al. *Band gap narrowing in Au-decorated Cr_2O_3 films*. Journal of Applied Physics, 2022, 132, 045302.
- [25] A. Rahman, et al. *Electrical transport properties of Au-doped metal oxide thin films*. Solid State Sciences, 2023, 142, 107246.